

Microbiological Communication

Comparative Investigation on Micro-Structural, Morphological, Optical, Magnetic and Anti-Microbial Traits of Undoped and Nickel-Incorporated Zinc Oxide Nanoparticles

Mary Clementia I¹ and K. Raji²

Post Graduate and Research Department of Physics, Holy Cross College, (Autonomous) Tiruchirappalli, Tamil Nadu, India

ABSTRACT

The main objective of the present work is to synthesize pure and nickel doped zinc oxide nanoparticles by facile co precipitation technique. The work is confined to study the effect of various weight ratios (0.3, 0.6, 0.9) % Nickel into Zinc oxide and to witness the drastic changes that occur in its various physical properties such as structural, optical, magnetic from X ray diffraction (XRD), UV visible (ultra violet) spectra, VSM (Vibrating sample magneto meter). XRD analysis reveals the wurtzite hexagonal structure and it is also found that as the doping concentration increases the crystallite size decreases from 4.6 nm to 3.0 nm. SEM results depicts the agglomeration of the particle, the synthesized samples shows both rod and flakes formation when the doping concentration is increased. Morphological changes were analysed TEM (Transmission electron microscope). The enhancement in the optical behaviour were observed and the energy band gap is calculated with the data obtained from UV-Visible spectra and the optical properties shows a tremendous increase as the Ni content increases which proves the sample a suitable candidate for solar cells and photovoltaic devices. Purity of the prepared sample were investigated through EDAX analysis. The hysteresis loop from the VSM analysis elucidate the saturation magnetization and the ferromagnetic behaviour of the sample. X-ray Photoemission Spectroscopy results indicates the presence of several oxygen species adsorbed on the surface. The study is also extended to analyse its anti-microbial effect against Staphylococcus aureus. The cell culture dish of the sample showed a notable resistance against Staphylococcus aureus when the concentration of nickel is increased and could be extended to pharmaceutical applications in treating several skin infections.

KEY WORDS: ANTI- MICROBIAL, CO-PRECIPITATION, NICKEL DOPING, OPTICAL PROPERTY, PHOTOVOLTAIC DEVICES.

INTRODUCTION

Over few years the usage of nanoparticles based on metals and their oxides have drawn a great interest almost in all the fields. Zinc oxide is a multifunctional II-VI group semiconductor grabbing a centre of attention to researchers due to its fascinating properties like wide band gap of 3.37 eV at room temperature, large exciton binding energy (60 meV), high optical transparency, high surface stability, large electrochemical coupling coefficient and strong excitonic emission etc. It is obvious that both Ni and Zn have the same valence with same structure which is because the ionic radii

of both Ni²⁺ (0.69 Å) and Zn²⁺ (0.74 Å) are very closer (Perna et al. 2020; Gudkov et al. 2021).

It is reported that Ni²⁺ could be easily replaced by Zn²⁺ in Zinc oxide lattice without changing its hexagonal structure, thus making Nickel doped Zinc oxide nanoparticles a promising material in the field of optoelectronic devices with its enormous optical and magnetic properties (Chattopadhyay et al. 2019; Ali et al. 2020). Observing at this point of view, this Zinc oxide which is in the form nanostructured powders could exhibit great efficiency in innumerable performances including gas sensors, solar cells and photo catalyst with high chemical activity. Generally the oxygen deficient off-stoichiometric of Zinc oxide possess a wide n-type conductivity, but a tremendous enhancement in its conductivity is noticed when dopant is added (Akdağ et al. 2016; Anandan et al. 2016; Uma et al. 2019).

Article Information: *Corresponding Author: maryclementia@hctrichy.ac.in

Received 15/09/2021 Accepted after revision 15/12/2021

Published: 31st December 2021 Pp- 1813-1820

This is an open access article under Creative Commons License,

Published by Society for Science & Nature, Bhopal India.

Available at: <https://bbrc.in/> DOI: <http://dx.doi.org/10.21786/bbrc/14.4.64>

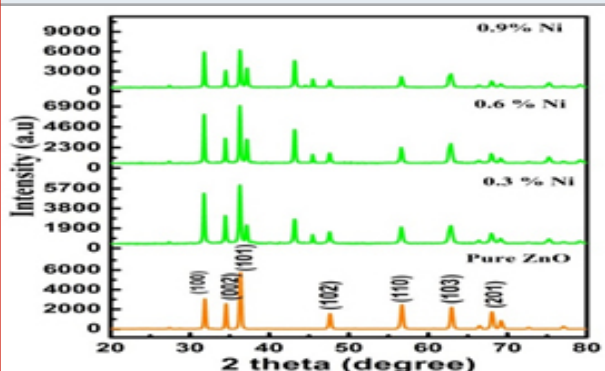
Here in this investigation undoped and nickel doped Zinc oxide nanoparticles were actualized by a very simple yet effective coprecipitation method. The main objective of this work is to study the morphological, optical and ferromagnetic behaviour of undoped and Nickel doped Zinc oxide nanoparticles with variation in the doping concentration (Ahmad 2019; Ali et al. 2020).

MATERIAL AND METHODS

Analytical grade reagents of Zinc acetate dihydrate $Zn(CH_3CO_2)_2$, sodium hydroxide (NaOH), and Nickel chloride ($NiCl_2$) with purity of 99.7%, were used in the formation of undoped and Nickel doped zinc oxide nanoparticles. During the process, the stemware was well covered in order to prevent contamination and evaporation of ethanol. A solution of 0.5 mole $Zn(CH_3CO_2)_2$ was prepared by dissolving (54.877g) in 450 ml of double distilled water and 0.5 mole of NaOH prepared by dissolving (20g) in 50 ml of double distilled water. The so formed solution of NaOH was introduced into the $Zn(CH_3CO_2)_2$ solution drop-wisely under constant strenuous stirring to avoid cluster formation. The impurities in the precipitate were separated by rinsing repeatedly with double distilled water and annealed at 600 °C for two hours in a muffle furnace to acquire the undoped Zinc oxide nanoparticles.

Nickel doped Zinc oxide nanoparticles were formed by taking equal weight of $Zn(CH_3CO_2)_2$ and NaOH were dissolved in 450 ml of double distilled water. Nickel II chloride ($NiCl_2 \cdot 6H_2O$) were taken in the varying concentration (0.3, 0.6, 0.9 %) was dissolved separately in 50 ml of water and then added to the solution containing Zinc acetate dihydrate $Zn(CH_3CO_2)_2$ and NaOH. The final solution was then allowed to remain in constant stirring for 2 hours. Then left overnight for sedimentation. Then the solution was carefully removed and subjected to centrifuge for further removal of impurity. The powder was annealed at a temperature of 600 °C in muffle furnace for 1 hour.

Figure 1: XRD pattern of undoped and Nickel doped Zinc oxide nanoparticles



For the characterization techniques, the formation of the hexagonal wurzite structure of the prepared particles were determined by X-ray diffractometer. Surface morphology were visualized by both SEM and TEM. The spectra of the photocatalysis absorbance were measured by a UV-Vis

spectrophotometer. Elemental composition, chemical and electronic state exist within the material were found by XPS and EDAX studies. The ferromagnetic behaviour was found from VSM analysis.

RESULTS AND DISCUSSION

XRD Analysis: The hexagonal wurtzite structure of the so prepared nanoparticles was confirmed by the XRD pattern and crystallite size was estimated by Debye-Scherrer method. Figure 1 exhibits the X-ray pattern of undoped and Nickel doped Zinc oxide nanoparticles.

XRD pattern shows that all the obtained peaks of Nickel substituted Zinc oxide nano crystals were incredibly matches well with the Joint Committee on Powder diffraction Standards (JCPDS) for ZnO (Card No. 36-1451, $a = b = 3.2498 \text{ \AA}$ and $c = 5.2066 \text{ \AA}$) which could be indexed as the hexagonal wurtzite structure of Zinc oxide. As the doping concentration was increased the intensity and variation of the position peak were also increased. This changes in peaks position indicates that nickel is substituted in the Zinc oxide lattice without any impurity phase (Danial 2020; Al-Ariki et al. 2021).

But the inclusion of the dopants produced defects in the crystal lattice of Zinc oxide which resulted in its change in size of the sample. The average crystallite sizes (D) of the prepared nanoparticles were calculated by Scherrer's equation

$$D = \frac{0.9 \lambda}{B \cos \theta} \quad (1)$$

where 'D' implies the crystallite size, ' λ ' implies the wavelength of radiation exposed, ' θ ' implies the Bragg angle and 'B' implies full width at half maxima (Belkhaoui et al. 2019; Priya et al. 2021).

It is seen from the above figure 1 that all the prepared nanoparticles have their dominant peak congruent to (102). To calculate the crystallite size three predominant peaks (002), (101), (102) were considered. The crystallite size of undoped and Nickel doped Zinc oxide is tabulated in table 1. It is worthy to note that the diffraction peaks get more intense at the same time becomes narrower as the annealing temperatures was increased indicating the formation of a good crystalline structure. It is also evident that the crystallite size was increased as the concentration of the dopants was raised which proved the impact of the dopants (Wang 2019).

Optical properties: UV-Visible Analysis: Ultra Violet-Vis analysis was used to measure the diminution of a beam of light that occurred after passing through or gets reflected back from a sample surface. Nickel doped Zinc oxide showed higher transparency in the visible regions at around 480 nm and the lowest transparency in wavelength smaller than 380 nm in comparison to the undoped and Nickel doped Zinc oxide nanoparticles. While comparing all samples, Nickel doped Zinc oxide nanoparticles exhibited

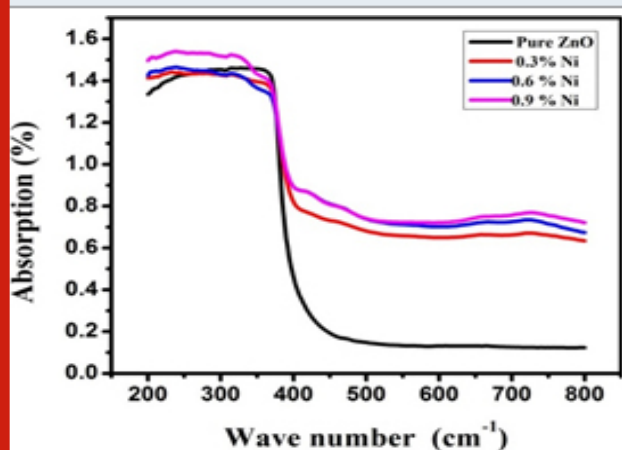
the highest absorption within the wavelength smaller than 400 nm. The absorption spectra of undoped and Nickel

doped zinc oxide nanoparticles is shown in Figure. 2 (Nallusamy and Nammalvar 2019).

Table 1. Crystallite size of pure and Ni doped ZnO nanoparticles

| Compound | Annealing Temperature °C | d spacing | θ (radians) | crystallite size(nm) |
|-----------|--------------------------|-----------|--------------------|----------------------|
| Pure ZnO | 600 °C | 2.3333 | 0.32375 | 4.68394E-08 |
| Ni (0.3%) | | 2.3333 | 0.3235 | 3.93042E-08 |
| Ni (0.6%) | | 2.6666 | 0.2981 | 3.80981E-08 |
| Ni (0.9%) | | 2.8808 | 0.27143 | 3.04412E-08 |

Figure 3: Absorption spectra of undoped and Nickel doped Zinc oxide nanoparticles

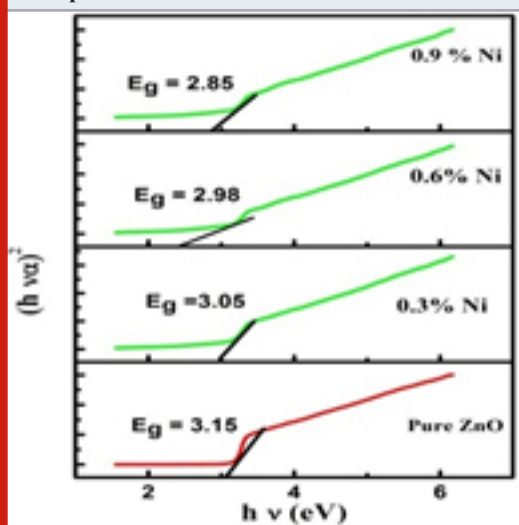


colour exhibited by the semiconductor nanoparticles would be usually due to the to this surface plasmon resonance. Thus by subjecting the sample to UV-Vis spectroscopy upon chromatographic separation, the unique optical properties could be detected and the formation of the nanoparticles could also be found out (Ghosh 2019).

The band gap was calculated by plotting $(\alpha h\nu)^2$ versus the photon energy ($h\nu$), and by extrapolating the intercept of the curve to zero absorption in the photon energy axis which is shown in Figure 3(b). The band gap energies of Nickel doped Zinc oxide nanoparticles were found to be smaller than that of undoped Zinc oxide nanopowder which may be due to the effect of Nickel concentrations (Vidhya et al. 2021).

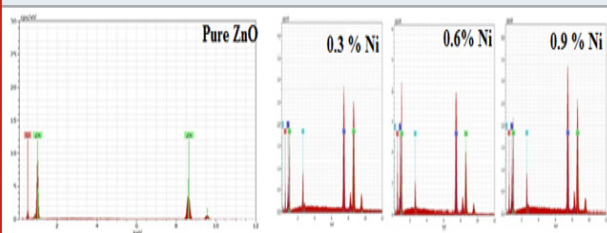
EDAX Analysis: The elemental composition of the synthesized sample of undoped and Nickel doped Zinc oxide was determined by EDAX spectra and shown in Figure4.

Figure 3(b): Band gap of pure and Ni doped ZnO nanoparticles



When the sample was brought under the influence of the electromagnetic field, the electron presents in the valence band experienced coherent oscillation, which in turn triggered the metallic nanoparticles to absorb electromagnetic radiations. This resonance is known as surface plasmons which occur only with nanoparticles and varies accordingly to its formations. Thus the size and the

Figure 4: EDAX of undoped and Nickel doped Zinc oxide nanoparticles



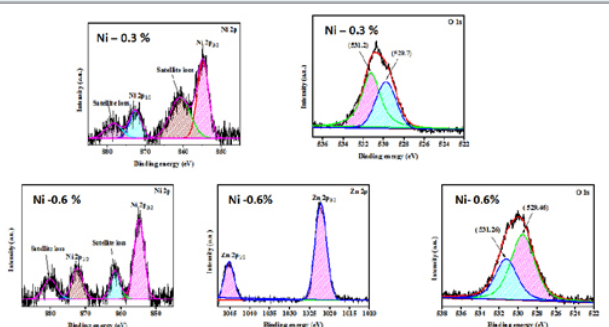
The existence of zinc, oxygen, Nickel and other elements without any impurity was confirmed from the above Figure 4. The pattern showed that the prepared Zinc oxide sample had the elemental composition of Nickel doped Zinc oxide nanoparticles shown in Table 3 (Kumari et al. 2021).

XPS Analysis: XPS analysis is a perceptive characterization approach for reviewing the chemical constitution and the valence states of substances embodied in the prepared nanoparticles. Figure 5 shows the survey spectrum and core level spectrum of Zn and O atoms of Nickel doped Zinc oxide nanoparticles, for 0.3% and 0.6% concentration respectively. The XPS peak of Nickel doped Zinc oxide nanoparticles is featured in Figure 5.

Table 3. Elemental composition of undoped and Nickel doped Zinc oxide nanoparticles

| Annealing T° C 600°C | Element | Series | Atomic Weight (Weight %) | Uncertainty Count (Weight %) | K factor (Weight %) |
|-------------------------|---------|-----------|-----------------------------|---------------------------------|------------------------|
| Pure ZnO | O | | 62.46 | 28.93 | 5.57 |
| | Zn | | 37.54 | 71.07 | 1.79 |
| 0.3 % of Ni | Zn | K- Series | 35.56 | 51.66 | 1.52 |
| | O | | 34.38 | 12.22 | 3.96 |
| | Ni | | 24.13 | 31.46 | 0.94 |
| | Cl | | 5.92 | 4.66 | 0.28 |
| 0.6 % of Ni | | K- Series | | | |
| | O | | 58.50 | 27.48 | 6.58 |
| | Ni | | 21.56 | 37.55 | 1.05 |
| | Zn | | 16.64 | 27.12 | 1.05 |
| 0.9 % of Ni | | | | | |
| | O | | 38.86 | 14.50 | 4.69 |
| | Zn | | 30.37 | 46.31 | 1.47 |
| | Ni | | 25.37 | 34.73 | 1.07 |
| | Cl | | 5.40 | 4.47 | 0.29 |

Figure 5: XPS peak of Nickel doped Zinc oxide nanoparticles



Doublet peak shown in the Figure 5 which corresponds to the core level spectra of Zn2p_{1/2} and Zn2p_{3/2} ions of ions is shown. The binding energy of Zn2p_{3/2} and Zn2p_{1/2} orbitals appeared at (531.2 eV, 529.7 eV), (531.26 eV, 529.46eV) which corresponded to ZFLi, ZFNa and ZFK NPs. The doublet peak of the binding energy was transfigured towards the lower energy region when Nickel dopant was added. Thus, the divalent state of Zn ions was confirmed by the difference in the position of the doublet peaks from which the spin split value was calculated (Kezhen et al. 2020; Maleki et al. 2021).

Morphology Analysis: The morphology of ZnO-xNi (x = 0.3, 0.6 and 0.9) as-synthesized nanocrystals were investigated with High resolution transmission electron microscopy (HR-TEM) and shown in Figure 6. Selected area electron diffraction (SAED) patterns were also presented. HR-TEM images displayed two types of morphologies, slightly rectangular and cubic. The

nanoparticles were arbitrarily selected from the micrograph in order to measure the particle-size distribution via image J. Figure 6 showcase the TEM images of the Nickel doped Zinc oxide nanoparticles at a concentration of 0.3, 0.6 and 0.9 % by weight. This particle distribution plays a vital role in determining the magnetic behaviour of the sample also provides the information regarding the coupling of spin (Sa- nguanprang et al. 2019; Naskar et al. 2020).

Figure 6: TEM image with SAED pattern of undoped and Nickel doped Zinc oxide nanoparticles

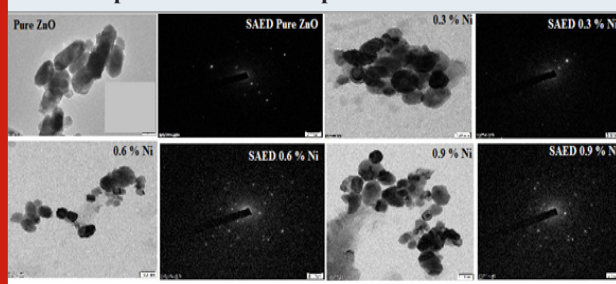
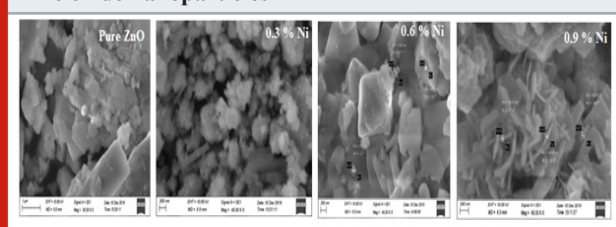
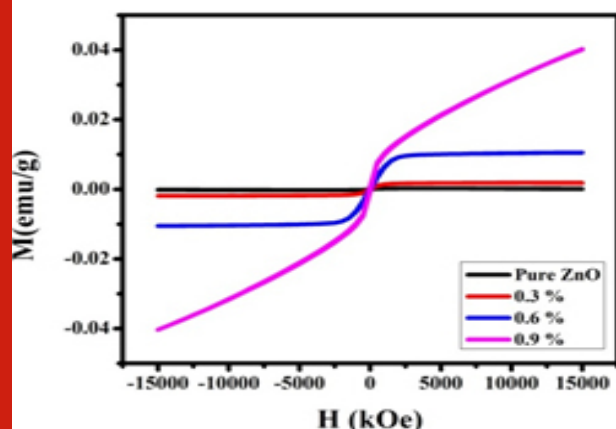


Figure 7: SEM topography of undoped and Nickel doped Zinc oxide nanoparticles



SEM Analysis: The formation of the particle in the nano range was confirmed from the SEM images shown in Figure 7 which were in good accordance with the particle size estimated from the XRD pattern depicted in the Figure 7 that the particles were spherical in shape.

Figure 8: M-H curve of undoped and Nickel doped Zinc oxide nanoparticles



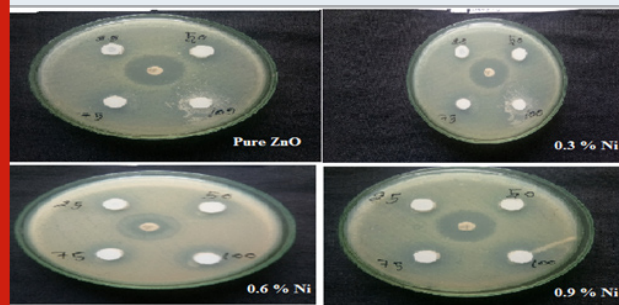
From the results obtained, it was seen that that the prepared sample powders were in nano range with a very low dimensions and the size varied with the increase in the Nickel content. It was also observed that while increasing the Nickel doping, the size of nanoparticles was decreased slightly which was already proved by the crystallite size calculation from XRD pattern in above section. Hence the SEM outcomes were in good correlation with XRD pattern, which was well defined that there was a decrease in the particle size as the concentration of the dopants was increased. Zinc oxide when doped with Nickel leads to nanopores which was shown in Figure 7 and it was seen as the doping concentration was increased resulted with the change in the formation exhibiting rod shaped into nano flakes indicated the effect of doping concentration (Beazer et al. 2021; Khan et al. 2021).

VSM Analysis: The M-H loop of the synthesized nanoparticles were shown in Figure 8. The samples pass origin of coordinates, the remanent magnetization (M_r), and coercivity (H_c) were found to be zero. The saturation magnetization, retentivity, and the coercive force values were given in Table 3. It is evident from Figure 8 that a transition from the paramagnetic state to the ferromagnetism state occurred when doping concentration was increased.

Table 3. Various parameters obtained from VSM analysis

| Compound | doping concentration by weight (%) | Parameters | | | |
|----------|------------------------------------|---------------------------|-------------------------|---------------------|-----------------------|
| | | Magnetization M_s (emu) | Retentivity M_r (emu) | Squarness M_r/M_s | Coercivity H_c (Oe) |
| Pure ZnO | | 140.35 | 122 | 1.150 | 654 |
| Ni | 0.3 | 132.45 | 120 | 1.103 | 546 |
| | 0.6 | 127.25 | 116 | 1.096 | 335 |
| | 0.9 | 113.75 | 108 | 1.053 | 203 |

Figure 9: Zone of inhibition of undoped and Nickel doped Zinc oxide nanoparticles



The ferromagnetism of the Zinc oxide doped with Nickel nanoparticles could arise from two possible sources. One is extrinsic magnetism and the other is intrinsic magnetism. Extrinsic source includes the formation of clusters of transition elements or secondary phase. Exchange interactions come under intrinsic source of magnetism. The probability of ferromagnetism exhibition due to formation of secondary phases and metallic clusters was entirely ruled out in case of Nickel doped sample. It was observed

in the present work, that the oxygen mediated exchange interaction took place among the dopant ions (Ni) leading to the ferromagnetic behaviour and magnetic saturation of Nickel -doped zinc oxide samples (Jeyasubramanian et al. 2019; Satpathy et al. 2021).

It was evident from the XRD analysis that when Nickel was perfectly incorporated into the ZnO lattice. In view of the Ni^{3+} ions substituted into ZnO lattice, the origin of magnetism in the samples was due to the exchange interaction between local spin polarized electrons (such as the electrons of Ni^{3+} ions) and the conductive electrons. Such interaction could lead to the spin polarization of conductive electrons. Consequently, the spin-polarized conductive electrons underwent an exchange interaction with local spin-polarized electrons of Ni^{3+} ions. Thus, after a successive long-range exchange interaction, almost all Ni^{3+} ions exhibited the same spin direction, which resulted in the ferromagnetism of the material (Pallavi et al. 2019; Khalid et al. 2021).

Anti-microbial mechanism: Nickel incorporated Zinc oxide nanoparticles were tested for its anti-microbial

mechanism against gram positive *Staphylococcus Aureus*. Figure 9 shows the antimicrobial action of Nickel doped Zinc oxide nanoparticles for *Staphylococcus Aureus*. The zone of inhibition (mm) of gram positive were ordered in Table 4. which were maintained in nutrient broth.

The analysis of the biological activity of Nickel assisted Zinc oxide nanoparticles were tested for different organisms in sterilized petri dishes adopting agar diffusion technique

for the sample annealed at 600 °C. The nutrient agar ambience was processed by incapacitating at about 121 °C. It was then sterilized, aseptically engulfed in petri plates and permitted to densify. Each petri plates were swabbed with the bacterial broth using a sterilized twig. Then the wells were aseptically added with the organic solvent extracts of leaves. The cell culture dish was detected to spot its zone of inhibition incubated at 37 °C for 24 hrs. The MIC of Zinc oxide with Nickel was thus calculated.

Table 4. Inhibition zones against different *Staphylococcus aureus*

| SAMPLE | Zone of inhibition (mm/ml) of against <i>Staphylococcus aureus</i> | | | | |
|----------|--|---------|---------|-----------|----------|
| | 25 m/ml | 50mm/ml | 75 m/ml | 100 mm/ml | Dominion |
| Pure ZnO | 16 | 13 | 12 | 15 | 14 |
| 0.3 % Ni | 12 | 15 | 17 | 16 | 15 |
| 0.6 % Ni | 14 | 16 | 19 | 20 | 17 |
| 0.9 % Ni | 16 | 19 | 22 | 26 | 22 |

Table 4 indicate the zinc oxide nanoparticles doped with Nickel had moderate activity with the concentration of 75 and 100 mg/mL and the following values were observed with respect to the control, against *Staphylococcus aureus*. The growth of all the microbes was inhibited by undoped Zinc oxide and Nickel doped Zinc oxide MCs. An increase in ZOI with the increase in the Nickel doped Zinc oxide -MCs concentration was observed in Figure 9. According to the results, gram-positive microbes, were more sensitive to Nickel doped Zinc oxide -MCs. Then the pure ZnO and becomes still resistant with the increase in the doping concentration. Thus, from the above table it was clear that as the doping concentration was increased the sample showed a drastic improvement in resisting the bacteria *Staphylococcus aureus*. Hence nickel incorporated Zinc oxide could be employed in treating skin diseases (Silva et al. 2019; Khalid et al. 2021).

CONCLUSION

The findings of the present study determines that XPS studies has proved the Nickel dopant to be located exactly into the Zinc oxide lattice that does not alter the structure. The enhanced optical studies further proved that doping Nickel with Zinc oxide makes it a good candidate in the field of optoelectronic devices. Among transition metal, Zinc oxide when doped with Nickel could produce augmented changes without altering the structure leading to many applications. The anti-microbial mechanism of Nickel doped zinc oxide showed a strong resist against gram positive bacteria when the doping concentration was increased from 0.3 % to 0.9 % concentration by weight and could employed making ointment and lotions for treating skin diseases in pharmaceutical applications.

ACKNOWLEDGEMENTS

The study was financially supported by the Research Institute, SRM University, Chennai, Tamil Nadu, India; SEM Facility, Consultancy on Characterization of Nanomaterials

(CCN); Centre for Nanoscience & Nanotechnology, Department of Chemistry, The Gandigram Rural Institute – DU, Tamil Nadu, India and Central Instrumentation Facility, Pondicherry University, Pondicherry, India.

Conflict of Interests: Authors declare no conflict of interests to disclose.

REFERENCES

- Ahmad, I., (2019). Inexpensive and quick photocatalytic activity of rare earth (Er, Yb) co-doped ZnO nanoparticles for degradation of methyl orange dye. Separation and purification Technology, 227: 115726. DOI: <https://doi.org/10.1016/j.seppur.2019.115726>.
- Akdağ, A., Budak, H.F., Yılmaz, M. et al. (2016). Structural and morphological properties of Al doped ZnO nanoparticles. Journal of Physics: Conference Series, 707(1): 012020. DOI: <https://iopscience.iop.org/article/10.1088/1742-6596/707/1/012020>
- Al-Ariki, S., Yahya, N.A., Sua'ad, A. et al. (2021). Synthesis and comparative study on the structural and optical properties of ZnO doped with Ni and Ag nanopowders fabricated by sol gel technique. Scientific Reports, 11(1):1-11. DOI: <https://doi.org/10.1038/s41598-021-91439-1>
- Ali, M., Sharif, S., Anjum, S. et al. (2020). Preparation of Co and Ni doped ZnO nanoparticles served as encouraging nano-catalytic application. Materials Research Express, 6(12):1250d5. DOI: <https://iopscience.iop.org/article/10.1088/2053-1591/ab6383>
- Ali, M.Y., Khan, M.K.R., Karim, A.T., et al. (2020). Effect of Ni doping on structure, morphology and opto-transport properties of spray pyrolysed ZnO nano-fiber. Heliyon, 6(3):03588. DOI: <https://doi.org/10.1016/j.heliyon.2020>

e03588

- Anandan, M., Dinesh, S., Krishnakumar, N. et al. (2016). Influence of Co doping on combined photocatalytic and antibacterial activity of ZnO nanoparticles. *Materials Research Express*, 3(11):115009. DOI: <https://iopscience.iop.org/article/10.1088/2053-1591/3/11/115009>
- Bawazeer, T.M., Alsoufi, M.S., Shkir, M., et al. (2021). Excellent improvement in photocatalytic nature of ZnO nanoparticles via Fe doping content. *Inorganic Chemistry Communications*, 130:108668. DOI: <https://doi.org/10.1016/j.inoche.2021.108668>
- Belkhaoui, C., Mzabi, N., and Smaoui, H., (2019). Investigations on structural, optical and dielectric properties of Mn doped ZnO nanoparticles synthesized by co-precipitation method. *Materials Research Bulletin*, 111:70-79. DOI: <https://doi.org/10.1016/j.materresbull.2018.11.006>
- Chattopadhyay, S., Misra, K.P., Agarwala, A., et al. (2019). Dislocations and particle size governed band gap and ferromagnetic ordering in Ni doped ZnO nanoparticles synthesized via co-precipitation. *Ceramic International*, 45(17B):23341-23354. DOI: <https://doi.org/10.1016/j.ceramint.2019.08.034>
- Danial, E.N., Hjiri, M., Abdel-Wahab, M.S., et al. (2020). Antibacterial activity of In-doped ZnO nanoparticles. *Inorganic Chemistry Communications*, 122: 108281. DOI: <https://doi.org/10.1016/j.inoche.2020.108281>
- Ghosh S.S., Choubey, C., and Sil, A., (2019). Photocatalytic response of Fe, Co, Ni doped ZnO based diluted magnetic semiconductors for spintronics applications. *Super Lattices and Microstructures*, 125:271-280. DOI: <https://doi.org/10.1016/j.spmi.2018.10.028>
- Gudkov, S.V., Burmistrov, D.E., Serov, D.A., et al. (2021). A Mini Review of Antibacterial properties of ZnO nanoparticles. *Front. Phys.*, 9: 641481. DOI: <https://doi.org/10.3389/fphy.2021.641481>
- Jeyasubramanian, K., William, R.V., Thiruramanathan, P., et al. (2019). Dielectric and magnetic properties of nanoporous nickel doped zinc oxide for spintronic applications. *Journal of Magnetism and Magnetic materials*, 485:27-35. DOI: <https://doi.org/10.1016/j.jmmm.2019.04.032>
- Khalid, A., Ahmad, P., Alharthi, A.I. et al. (2021). Enhanced Optical and Antibacterial Activity of Hydrothermally Synthesized Cobalt-Doped Zinc Oxide Cylindrical Microcrystals. *Materials*, 14(12):3223. DOI: <https://doi.org/10.3390/ma14123223>
- Khan, M.I., Fatima, N., Shakil, M., et al. (2021). Investigation of in-vitro antibacterial and seed germination properties of green synthesized pure and nickel doped ZnO nanoparticles. *Physics B: Condensed Matter*, 601(412563). DOI: <https://doi.org/10.1016/j.physb.2020.412563>
- Kumari, P., Misra, K.P., Chattopadhyay, S., et al. (2021). A brief review on transition metal ion doped ZnO nanoparticles and its optoelectronic applications. *Materials Today Proceedings*, 43(5):3297-3302. DOI: <https://doi.org/10.1016/j.matpr.2021.02.299>
- Maleki, A., Seifi, M., and Marzban, N., (2021). Evaluation of Sonocatalytic and Photocatalytic Processes Efficiency for Degradation of Humic Compounds Using Synthesized Transition-Metal-Doped ZnO Nanoparticles in Aqueous Solution. *Journal of Chemistry*, 2021. DOI: <https://doi.org/10.1155/2021/9938579>
- Nallusamy, S., and Nammalvar, G., (2019). Enhancing the saturation magnetisation in Ni doped ZnO thin films by TOPO functionalization. *Journal of Magnetism and Magnetic materials*, 485:297-303. DOI: <https://doi.org/10.1016/j.jmmm.2019.04.089>
- Naskar, A., Lee, S., and Kim, K.S., (2020). Antibacterial potential of Ni-doped zinc oxide nanostructure: Comparatively more effective against Gram-negative bacteria including multi-drug resistant strains. *RSC Advances*, 10(3):1232-1242. DOI: <https://doi.org/10.1039/C9RA09512H>
- Prerna, Arya, S., Sharma, A., et al. (2020). Morphological and Optical Characterization of Sol-Gel Synthesized Ni-Doped ZnO Nanoparticles. *Integrated Ferroelectrics*, 205(1):1-14. DOI: <https://doi.org/10.1080/10584587.2019.1674992>
- Priya, R., Sahay, P., Saxena, N., et al. (2021). Systematic study of Ni, Cu co-doped ZnO nanoparticles for UV photodetector application. *Journal of Materials Science: Materials in Electronics*, 32(2):2011-2025. DOI: <https://doi.org/10.1007/s10854-020-04968-2>
- Qi, K., Xing, X., Zada, A., et al. (2020). Transition metal doped ZnO nanoparticles with enhanced photocatalytic and antibacterial performances: Experimental and DFT studies. *Ceramic International*, 46(2):1494-1502. DOI: <https://doi.org/10.1016/j.ceramint.2019.09.116>
- Sa-nguanprang, S., Phuruangrat, A., Thongtem, T. et al. (2019). Synthesis, analysis, and photocatalysis of Mg-doped ZnO nanoparticles. *Russian Journal of Inorganic Chemistry*, 64(14):1841-1848.
- Satpathy, S.K., Panigrahi, U.K., Panda, S.K., et al. (2021). Structural, optical, antimicrobial and ferromagnetic properties of Zn_{1-x}LaxO nanorods synthesized by chemical route. *Journal of Alloys and Compounds*, 865:158937. DOI: <https://doi.org/10.1016/j.jallcom.2021.158937>
- Silva, B.L.D., Abuçafy, M.P., Manaia, E.B., et al. (2019). Relationship Between Structure And Antimicrobial Activity Of Zinc Oxide Nanoparticles: An Overview.

Int J Nanomedicine; 14:9395–9410. DOI: <https://doi.org/10.2147/IJN.S216204>

Uma, H.B., Ananda, S., and Nandaprakash, M.B., (2019). High efficient photocatalytic treatment of textile dye and antibacterial activity via electrochemically synthesized Ni-doped ZnO nano photocatalysts. Chemical Data Collections, 24:100301. DOI: <https://doi.org/10.1016/j.cdc.2019.100301>

Undre, P.G., Kharat, P.B., Kathare et al. (2019). Ferromagnetism in Cu 2+ doped ZnO nanoparticles and their Physical properties. Journal of Materials Science:

Materials in Electronics, 30:4014–4025. DOI: <https://link.springer.com/article/10.1007/s10854-019-00688-4>

Vidhya, M.S., Ameen, F., Dawoud, T., et al. (2021). Anti-cancer applications of Zr, Co, Ni-doped ZnO thin nanoplates. Materials Letters, 283:128760. DOI: <https://doi.org/10.1016/j.matlet.2020.128760>.

Wang, J., Zhou, Q., and Zeng, W., (2019). Competitive adsorption of SF₆ decompositions on Ni-doped ZnO (100) surface: Computational and experimental study. Applied Surface Science, 479:185- 197. DOI: <https://doi.org/10.1016/j.apsusc.2019.01.255>